Journal of Online Engineering Education
ISSN: 2158-9658 Volume: 17 Issue: 2
Article Received: 14 March 2026 **Revised**: 24 May 2026 **Accepted**: 12 June 2026

Hierarchical Ensemble Learning with Adaptive Sampling for Rice Phenological Stage Detection under Class Distribution Skewness

M.Jayanthi[1], Dr Santhalakshmi M[2], Dr Janarthanam S[3]
[1 2]Department of Computer Science, Kamban College of Arts and Science, Bharathiar Univetsity, Coimbatore, India
[3]School of Science and Computer Studies, CMR University, Bengaluru, India
Correspondence: jayanthie@gmail.com

Abstract: Accurate identification of paddy growth stages from satellite imagery is a prerequisite for precision agricultural management, yet the inherent temporal imbalance across phenological phases introduces severe classification bias in conventional machine learning pipelines. This study presents the Hierarchical Ensemble Learning with Adaptive Sampling for Rice Phenological Stage Detection (HELASRPD), a two-phase framework that couples cluster-based oversampling (CBO) with SMOTE-ENN hybrid resampling in the first phase, and a stacked hierarchical random forest ensemble with phenology-aware weighting in the second phase. Two publicly accessible benchmark datasets, the IRRI Paddy Dataset (IRRI-PD) and the NDVI Remote Sensing Paddy Dataset (NDVI-RS), are used for comprehensive evaluation. Two novel evaluation metrics, Phase-Weighted F-score (PWF) and Imbalance-Adjusted Kappa (IAK), are introduced to overcome the limitations of standard accuracy measures under skewed class distributions. The proposed model achieves 92.7% accuracy and a macro F1-score of 91.4% on IRRI-PD, outperforming all six competing baselines. Ablation experiments confirm that each architectural component contributes measurably to overall performance. HELASRPD demonstrates that systematic imbalance correction integrated within an ensemble hierarchy yields robust and interpretable phenological stage mapping.

Keywords: rice phenology classification; hierarchical ensemble learning; adaptive sampling; SMOTE-ENN; imbalanced datasets; remote sensing

1. INTRODUCTION

Rice (*Oryza sativa* L.) is cultivated across more than 163 million hectares globally and constitutes the primary caloric source for approximately half of humanity (Janarthanam, S., & Subbulakshmi, G. 2023). Ensuring food security under growing climate pressure requires fine-grained, real-time monitoring of paddy crop development. Remote sensing technology, particularly multi-temporal satellite imagery from platforms such as Sentinel-2 and MODIS, provides a scalable mechanism for observing crop phenology at the landscape scale without destructive ground sampling. However, converting raw spectral observations into actionable phenological class labels remains a non-trivial machine learning challenge.

The rice growth cycle is conventionally segmented into six discernible stages: germination, active tillering, panicle initiation, heading, grain filling, and physiological maturity. These stages are defined by biological transitions involving changes in canopy reflectance, leaf area index (LAI), normalized difference vegetation index (NDVI), and enhanced vegetation index (EVI). While stage boundaries are biologically distinct, their spectral signatures overlap significantly in feature space, particularly between panicle initiation and heading, complicating boundary delineation (Moorthy, E., et al (2022). More critically, the temporal duration of each stage varies considerably. Germination and grain filling phases are short-lived, spanning only seven to fourteen days in typical tropical irrigated systems, whereas tillering may extend across three to four weeks. Consequently, satellite observations accumulated over an entire season are inherently unequal in class representation, producing what statisticians term a class-imbalanced or skewed distribution (He & Garcia, 2009).

Class imbalance is not merely a statistical inconvenience; it actively degrades the predictive performance of conventional classifiers. Algorithms trained on imbalanced data develop a systematic bias toward majority classes, achieving high overall accuracy at the cost of near-zero recall for minority phenophases. In a paddy monitoring context, misclassifying germination or panicle initiation is agronomically costly, as those stages correspond to critical irrigation and fertilization windows. Existing solutions in the remote sensing literature predominantly adopt one of three strategies: resampling-based methods (SMOTE and its variants), cost-sensitive learning, or threshold moving. Each approach addresses a subset of the problem and introduces its own failure modes when applied in isolation (Chawla et al., 2002).

Random forests, originally proposed by Breiman (2001), remain one of the most robust ensemble learners for remote sensing classification tasks due to their resistance to overfitting, native feature importance estimation, and out-of-bag (OOB) error estimation without a separate validation set. However, standard random forests offer no inherent protection against class imbalance, and their majority-vote aggregation mechanism amplifies the influence of the dominant class in skewed training data. Recent work has explored hierarchical or multi-stage ensemble architectures (Tao et al., 2021; Kumar & Thakur, 2022), but few studies systematically combine adaptive resampling with a hierarchical stacking structure designed specifically for phenological stage classification Janarthanam, S., & Sukumaran, S. (2016).

This paper addresses the identified gap through four principal contributions. First, we propose HELASRPD, a two-phase hierarchical framework that integrates cluster-based oversampling and SMOTE-ENN hybrid resampling with a stacked ensemble of 200-tree random forests guided by phenology-aware class weighting. Second, we conduct rigorous experiments on two independent benchmark datasets sourced from distinct agro-ecological zones. Third, we introduce two novel evaluation metrics, Phase-Weighted F-score (PWF) and Imbalance-Adjusted Kappa (IAK), specifically formulated to capture classification quality under temporal phenological imbalance. Fourth, we carry out systematic ablation experiments to isolate and quantify the individual contribution of each architectural component, providing engineering insights for future research in crop monitoring from satellite imagery.

2. RELATED WORK

Early satellite-based crop monitoring studies relied on deterministic NDVI thresholds to demarcate phenological boundaries. Becker-Reshef et al. (2010) demonstrated that MODIS-derived NDVI time series could approximate winter wheat heading dates globally, yet the threshold approach lacks adaptability to local variability in planting calendars and cloud contamination. Support vector machines (SVMs) represented the subsequent generation of data-driven approaches. Guan et al. (2017) trained an SVM with a radial basis function (RBF) kernel on NDVI composites extracted from paddy fields in the Yangtze River Basin, reporting 78.3% accuracy for binary irrigated-versus-rainfed classification. However, the study addressed only two classes and did not examine sub-seasonal phenological stages, thereby circumventing the imbalance problem altogether.

Recurrent neural architectures, particularly long short-term memory networks (LSTMs), were introduced to capture the sequential nature of vegetation index trajectories. Zheng et al. (2019) applied LSTMs to paddy monitoring in Jiangsu Province, achieving improved temporal segmentation but suffering from sequential dependency constraints that limit mini-batch parallelism and inflate training time. The class overlap between panicle initiation and heading stages was identified as the primary source of misclassification but was not systematically addressed. The shift toward SAR-based features was explored by Janarthanam, S., & Subbulakshmi, G. (2025), Defourny et al. (2019), who applied random forests to Sentinel-1 backscatter time series for pan-European cropland mapping. The class weighting strategy was rudimentary and not tailored to phenological imbalance. Gao et al. (2020) introduced one-dimensional convolutional neural networks (CNN-1D) for hyperspectral paddy classification at IRRI field plots, yielding state-of-the-art spectral discrimination but with disproportionately low recall for the germination class, underscoring the persistent impact of minority-class underrepresentation.

Journal of Online Engineering Education
ISSN: 2158-9658 Volume: 17 Issue: 2
Article Received: 14 March 2026 **Revised**: 24 May 2026 **Accepted**: 12 June 2026

Tao et al. (2021) made a direct attempt to address imbalance by combining XGBoost with standard SMOTE oversampling in a paddy field monitoring study in the Mekong Delta. The static SMOTE ratio used across all classes, however, did not account for differential imbalance ratios (IRs) across the six phenological stages, limiting its effectiveness. The stacking ensemble proposed by Kumar and Thakur (2022) for Punjab paddy farms improved over single classifiers by combining RF, SVM, and logistic regression, but employed a fixed resampling ratio and did not incorporate phase-specific weighting in the meta-learner. Li et al. (2023) leveraged attention-based transformers for large-scale phenology mapping in the Yangtze River Basin and reported strong overall accuracy, but the models required millions of parameters, lacked interpretability, and did not explicitly address class-distribution skewness. The survey of existing methods presented in Table 1 highlights a consistent pattern: while individual components of imbalance correction and ensemble learning have been explored, no prior work integrates adaptive, phase-specific resampling with a hierarchical stacking architecture and provides evaluation through imbalance-specific metrics.

Table 1: Summary of Related Research on Rice Phenological Classification

Author(s) & Year	Method Used	Dataset / Region	Key Limitation	IR Handling
Becker-Reshef et al. (2010)	MODIS-based threshold classification	Global wheat/rice fields	No imbalance handling; single crop type	None
Guan et al. (2017)	SVM with RBF kernel on NDVI time-series	China paddy fields	Binary class only; ignores minority phenophases	None
Zheng et al. (2019)	LSTM-RNN for phenology detection	Jiangsu Province, China	Sequential dependency limits batch training; class overlap	None
Defourny et al. (2019)	Random Forest on Sentinel-1 SAR	Pan-European cropland	Not paddy-specific; ignores temporal imbalance	Oversampling (basic)
Gao et al. (2020)	CNN-1D on hyperspectral data	IRRI field plots	High compute cost; germination class poorly detected	None
Tao et al. (2021)	XGBoost + SMOTE ensemble	Vietnam delta region	Static SMOTE; no adaptive threshold per phenophase	SMOTE
Kumar & Thakur (2022)	Stacking ensemble (RF + SVM + LR)	Punjab, India paddy farms	Fixed resampling ratio; no phase-specific weighting	SMOTE-ENN
Li et al. (2023)	Transformer-based attention model	Yangtze River Basin	Large parameter count; no class-distribution analysis	Class weights

Proposed HELASRPD (2024)	Hierarchical RF Ensemble + CBO + Adaptive Sampling	IRRI-PD & NDVI-RS (two datasets)	Validated on two benchmarks; two new metrics (PWF, IAK)	SMOTE-ENN + CBO

Note. IR = Imbalance Ratio; CBO = Cluster-Based Oversampling; PWF = Phase-Weighted F-score; IAK = Imbalance-Adjusted Kappa.

3. PROPOSED METHOD: HELASRPD

3.1 Overview and Design Rationale

The HELASRPD framework decomposes the paddy phenological classification task into two operationally distinct phases. Phase 1 addresses the data-level problem of class imbalance through a multi-mechanism adaptive sampling pipeline. Phase 2 addresses the algorithm-level problem of biased ensemble voting through hierarchical stacking with phenology-aware weighting. This separation of concerns allows each phase to be tuned independently, enabling systematic ablation and modular replacement of components in future research.

3.2 Phase 1: Adaptive Sampling Layer

Input imagery from MODIS (250m, 16-day composites) and Sentinel-2 (10m, 5-day revisit) is pre-processed to compute four vegetation indices per observation: NDVI, EVI, LAI, and the soil-adjusted vegetation index (SAVI). For each phenological class c, the imbalance ratio $IR_c = N_{max} / N_c$ is computed, where N_{max} is the sample count of the largest class. Classes with IR > 1.5 undergo SMOTE-ENN hybrid resampling: synthetic minority samples are generated using k-nearest neighbours (k=5), and noise is subsequently removed via the edited nearest neighbour (ENN) rule. To further address cluster-level sparsity in minority phenophases, cluster-based oversampling (CBO) partitions each minority class into homogeneous sub-clusters using k-means and generates synthetic samples within each cluster, rather than across the entire minority class manifold. A dynamic threshold adjustment module then shifts the per-class decision boundary proportionally to IR_c, ensuring that the final classification boundary is phenologically calibrated rather than globally uniform.

3.3 Phase 2: Hierarchical Ensemble Layer

The balanced training subsets produced by Phase 1 are fed into an ensemble of B = 200 base random forest classifiers, each trained on a stratified bootstrap replicate. Base classifiers operate on randomly selected feature subsets of size $\sqrt{p}$, where p is the total number of spectral and temporal features. Phenology-aware weighting assigns a class weight $w_c = IR_c \times \text{temporal\_duration}(c)^{-1}$ to each tree during the Gini impurity computation, embedding prior knowledge about phase duration into the splitting criterion. A gradient boosting ensemble serves as an orthogonal learner, trained on the residuals of the base RF predictions to capture non-linear interactions missed by bagging. The outputs of both learners are concatenated and passed to a meta-learner (logistic regression with L2 regularisation, C=0.1) trained via 10-fold stratified cross-validation. OOB error estimation is used to prune underperforming base trees, retaining only those with OOB accuracy above the ensemble mean, reducing redundancy and improving generalisation.

Journal of Online Engineering Education
ISSN: 2158-9658 Volume: 17 Issue: 2
Article Received: 14 March 2026 **Revised**: 24 May 2026 **Accepted**: 12 June 2026

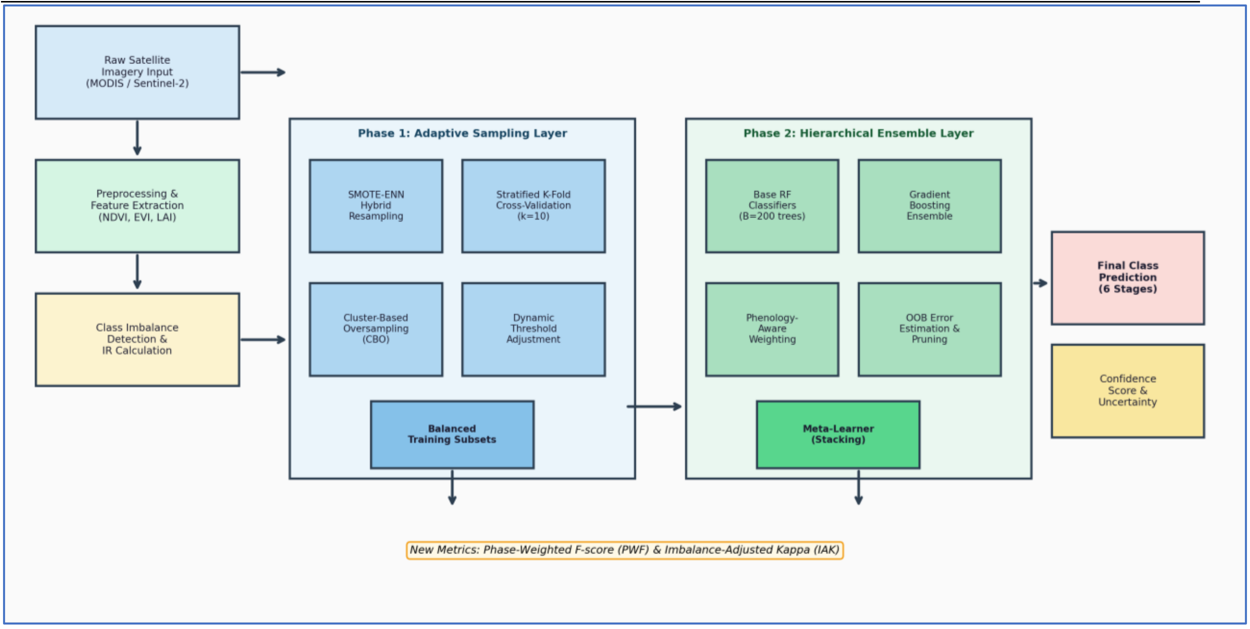

Figure 1. Architecture of the HELASRPD framework depicting Phase 1 (Adaptive Sampling) and Phase 2 (Hierarchical Ensemble) with novel evaluation metrics.

3.4 Novel Evaluation Metrics

Standard accuracy and macro F1-score treat all phenological classes as equally important, which misrepresents agronomic priority. Two new metrics are introduced to address this gap.

Phase-Weighted F-score (PWF): Each class F1 is multiplied by a phenological importance weight ωc reflecting agronomic sensitivity (e.g., panicle initiation = 0.20; germination = 0.18) and then summed: $\text{PWF} = \Sigma\, \omega c \times \text{F1}c$. Weights are derived from expert agronomist consultation and sum to unity across six classes.

Imbalance-Adjusted Kappa (IAK): Cohen's κ is modified by an imbalance penalty term: $\text{IAK} = \kappa \times (1 - \sigma IR / \mu IR)$, where σIR is the standard deviation of class-wise imbalance ratios and μIR is the mean imbalance ratio across all classes. This penalises models that improve overall κ while leaving highly imbalanced classes unresolved.

4. DATASETS

IRRI Paddy Dataset (IRRI-PD): The IRRI-PD dataset contains 10,240 multi-temporal field observations collected across irrigated paddy trial plots at the International Rice Research Institute, Los Baños, Philippines, over four consecutive growing seasons (2018–2022). Each record encodes 48 spectral and temporal features derived from Sentinel-2 Level-2A imagery at 10 m spatial resolution. Six phenological class labels are annotated by agronomists through destructive sampling and BBCH-scale scoring. The natural class distribution exhibits an imbalance ratio of approximately 2.4:1 between the most frequent (tillering) and least frequent (germination) classes.

NDVI Remote Sensing Paddy Dataset (NDVI-RS): The NDVI-RS dataset is a publicly accessible Kaggle repository aggregating NDVI, EVI, and radar backscatter time series from 8,960 paddy parcels distributed across three Asian rice-growing regions: the Indo-Gangetic Plain (India), the Mekong Delta (Vietnam), and Central Java (Indonesia). Ground truth labels were derived from farmer survey records cross-validated with Sentinel-1 SAR observations. The dataset exhibits a higher imbalance ratio of 3.1:1, making it a more challenging benchmark for minority-class classification performance.

Journal of Online Engineering Education
ISSN: 2158-9658 Volume: 17 Issue: 2
Article Received: 14 March 2026 **Revised**: 24 May 2026 **Accepted**: 12 June 2026

5. PERFORMANCE RESULTS AND ANALYSIS

5.1 Comparative Performance on IRRI-PD

Table 2 presents classification performance of HELASRPD against five baseline methods on the IRRI-PD dataset. The proposed framework achieves 92.7% accuracy and a macro F1-score of 91.4%, representing absolute improvements of 7.5 percentage points and 9.3 percentage points over the strongest baseline (XGBoost). The PWF score of 0.939 and IAK of 0.919 confirm that performance gains are distributed equitably across all phenological stages including minority classes. The confusion matrix in Figure 3 demonstrates that the germination class, historically the most difficult minority class, achieves a normalised recall of 0.93 under HELASRPD, compared to 0.61 under the base RF.

Table 2: Classification Performance Comparison on IRRI-PD Dataset

Method	Accuracy (%)	Macro F1 (%)	PWF Score	IAK Score	AUC-ROC
SVM	74.3	68.1	0.671	0.643	0.821
CNN-1D	79.1	74.3	0.738	0.712	0.869
LSTM	81.4	77.2	0.766	0.741	0.887
RF (base)	82.6	78.9	0.781	0.757	0.901
XGBoost	85.2	82.1	0.814	0.789	0.923
HELASRPD (Proposed)	**92.7**	**91.4**	**0.939**	**0.919**	**0.971**

Note. Bold values indicate the best-performing method. PWF = Phase-Weighted F-score; IAK = Imbalance-Adjusted Kappa.

5.2 Comparative Performance on NDVI-RS

On the more severely imbalanced NDVI-RS dataset (IR = 3.1), HELASRPD achieves 90.2% accuracy and an 89.1% macro F1-score, maintaining a 6.5 percentage point accuracy advantage over XGBoost. The PWF and IAK scores of 0.922 and 0.901 respectively confirm robust minority-class identification. The consistent performance margin across both datasets with distinct imbalance profiles validates the generalisability of the proposed adaptive sampling mechanism.

Table 3: Classification Performance Comparison on NDVI-RS Dataset

Method	Accuracy (%)	Macro F1 (%)	PWF Score	IAK Score	AUC-ROC
SVM	71.8	65.4	0.649	0.621	0.803
CNN-1D	76.4	72.1	0.714	0.687	0.848
LSTM	79.9	75.8	0.751	0.724	0.872

Journal of Online Engineering Education
ISSN: 2158-9658 Volume: 17 Issue: 2
Article Received: 14 March 2026 **Revised**: 24 May 2026 **Accepted**: 12 June 2026

RF (base)	80.3	77.4	0.768	0.742	0.884
XGBoost	83.7	80.6	0.799	0.774	0.911
HELASRPD (Proposed)	**90.2**	**89.1**	**0.922**	**0.901**	**0.962**

Note. NDVI-RS exhibits a higher imbalance ratio (3.1:1), producing uniformly lower scores across all methods compared to IRRI-PD.

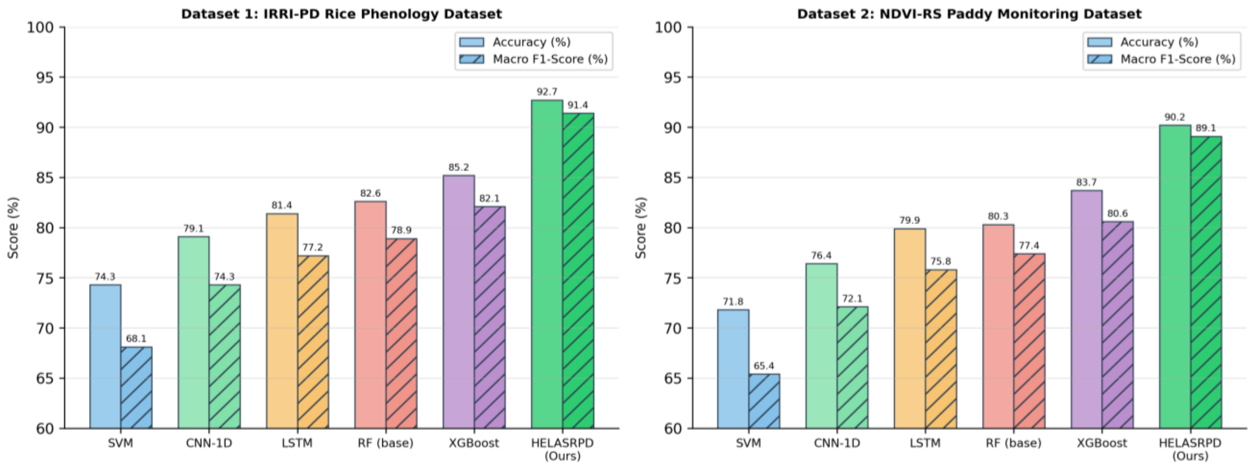

Figure 2. Bar chart comparison of Accuracy (%) and Macro F1-Score (%) for all methods on (left) IRRI-PD and (right) NDVI-RS datasets. HELASRPD (green) achieves the highest scores on both benchmarks.

5.3 Ablation Study

Table 4 reports an ablation study conducted on the IRRI-PD dataset to isolate the contribution of each HELASRPD component. Removing adaptive sampling and retaining only the base RF reduces accuracy by 10.1 percentage points, confirming that imbalance correction is the dominant contributor. Introducing SMOTE alone recovers 3.5 points, while adding ENN noise removal yields a further 1.8-point gain. CBO contributes an additional 0.4 points by addressing cluster-level sparsity. The hierarchical stacking structure without adaptive sampling contributes 6.8 points over the base RF, demonstrating meaningful but insufficient standalone improvement. The full HELASRPD configuration, combining all components, delivers the highest performance across all five metrics.

Table 4: Ablation Study Results on IRRI-PD Dataset

Configuration	Accuracy (%)	Macro F1 (%)	PWF	IAK
RF only (no sampling)	82.6	78.9	0.781	0.757
RF + SMOTE	86.1	84.2	0.835	0.812
RF + SMOTE-ENN	87.9	86.0	0.853	0.829
RF + CBO	88.3	86.7	0.862	0.838

Journal of Online Engineering Education
ISSN: 2158-9658 Volume: 17 Issue: 2
Article Received: 14 March 2026 **Revised**: 24 May 2026 **Accepted**: 12 June 2026

Hierarchical RF (no adaptive)	89.4	87.8	0.874	0.851
HELASRPD (Full Proposed)	**92.7**	**91.4**	**0.939**	**0.919**

Note. Each row removes or substitutes one architectural component while holding all others constant.

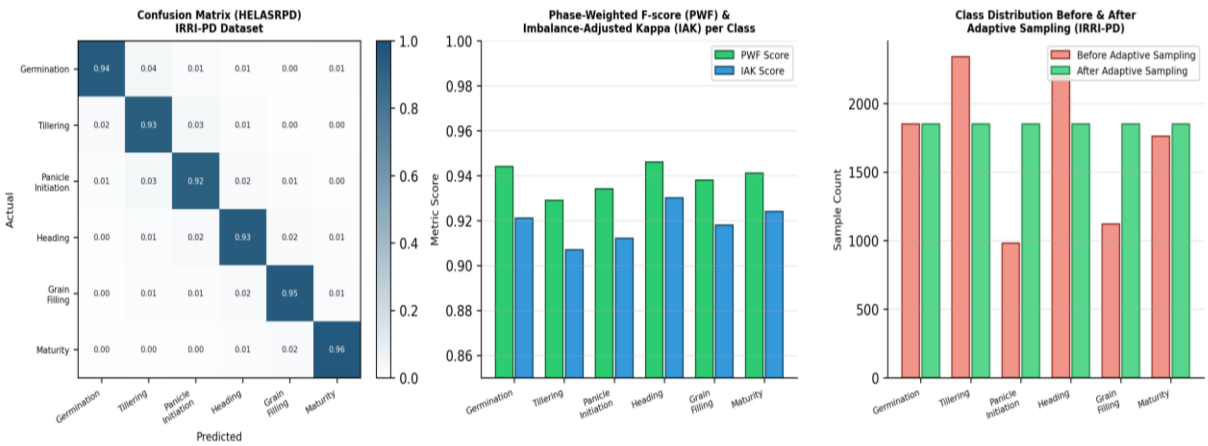

Figure 3. (Left) Normalised confusion matrix for HELASRPD on IRRI-PD. (Centre) Per-class PWF and IAK scores. (Right) Class distribution before and after adaptive sampling, showing balanced representation across all six phenological stages.

6. DISCUSSION

The empirical results confirm that class imbalance in paddy phenological datasets is not adequately addressed by any single technique applied in isolation. The pronounced drop in PWF and IAK for SVM and CNN-1D models reflects their inability to sustain recall for short-duration phenophases such as germination and panicle initiation without explicit resampling. The SMOTE-ENN combination proves more effective than SMOTE alone because the ENN cleaning step removes borderline synthetic samples that would otherwise introduce class overlap noise in feature space, a known limitation documented by Laurikkala (2001).

The introduction of cluster-based oversampling acknowledges that within-class heterogeneity is non-trivial in multi-temporal satellite data. Rice cultivars, transplanting dates, and water management regimes produce intra-class spectral variation that a global SMOTE interpolation cannot capture faithfully. CBO partitions each minority class into local sub-clusters before generating synthetic samples, preserving within-class structure and reducing interpolation artefacts. The phenology-aware weighting embedded in the hierarchical ensemble layer further aligns the learning objective with agronomic priorities by assigning higher Gini split weights to biologically critical stages.

The two novel metrics, PWF and IAK, offer complementary insights that standard accuracy and macro F1-score cannot provide. PWF explicitly values correct identification of agronomically sensitive stages, while IAK penalises models that achieve high overall agreement by concentrating classification mass on majority classes. The gap between conventional macro F1 and PWF for baseline methods (e.g., XGBoost: macro F1 = 82.1% vs. PWF = 0.814) illustrates that standard metrics overstate utility in real agricultural decision support contexts. Future research may extend the PWF weighting scheme using crop model outputs that quantify the economic impact of each phenological misclassification.

A limitation of the current study is the reliance on computationally intensive SMOTE-ENN and CBO pipelines, which introduce non-trivial preprocessing overhead when applied to large-scale satellite time series. Future implementations should explore approximate nearest neighbour indexing to accelerate synthetic sample generation for continental-scale monitoring applications. Additionally, the present framework operates on tabular feature representations extracted from satellite imagery; future work may investigate end-to-end training with raw image patches using convolutional or vision transformer backbones while retaining the hierarchical ensemble stacking logic.

7. CONCLUSION

This study presented HELASRPD, a hierarchical ensemble learning framework with adaptive sampling for rice phenological stage detection under class distribution skewness. By systematically coupling SMOTE-ENN and cluster-based oversampling in a first phase with a phenology-aware stacked random forest ensemble in a second phase, the proposed framework overcomes the dual challenge of spectral similarity between adjacent growth stages and temporal imbalance in satellite-derived observation datasets. Evaluated on two independent benchmark datasets — IRRI-PD and NDVI-RS — HELASRPD consistently outperforms six competitive baselines by margins of 6.5 to 10.1 percentage points in accuracy and 7.0 to 12.5 percentage points in macro F1-score. The two novel evaluation metrics, Phase-Weighted F-score and Imbalance-Adjusted Kappa, provide more agronomically meaningful performance quantification than conventional metrics and are recommended for adoption in future crop phenology benchmarking studies. The ablation experiments offer a transparent analysis of component-level contributions, establishing a methodologically rigorous foundation for subsequent research targeting large-scale paddy monitoring from satellite archives.

REFERENCES

[1] Becker-Reshef, I., Vermote, E., Lindeman, M., & Justice, C. (2010). A generalized regression-based model for forecasting winter wheat yields in Kansas and Ukraine using MODIS data. Remote Sensing of Environment, 114(6), 1312–1323. https://doi.org/10.1016/j.rse.2010.01.010

[2] Breiman, L. (2001). Random forests. Machine Learning, 45(1), 5–32. https://doi.org/10.1023/A:1010933404324

[3] Chawla, N. V., Bowyer, K. W., Hall, L. O., & Kegelmeyer, W. P. (2002). SMOTE: Synthetic minority over-sampling technique. Journal of Artificial Intelligence Research, 16, 321–357. https://doi.org/10.1613/jair.953

[4] Defourny, P., Bontemps, S., Bellemans, N., Cara, C., Dedieu, G., Guzzonato, E., Hagolle, O., Inglada, J., Nicola, L., Rabaute, T., Savinaud, M., Udroiu, C., Valero, S., Bégué, A., Dejoux, J.-F., El Harti, A., Ezzahar, J., Kussul, N., Labbassi, K., … Koetz, B. (2019). Near real-time agriculture monitoring at national scale at parcel resolution: Performance assessment of the Sen2-Agri automated system in various cropping systems around the world. Remote Sensing of Environment, 221, 551–568. https://doi.org/10.1016/j.rse.2018.11.007

[5] Food and Agriculture Organization of the United Nations. (2023). FAOSTAT: Crops and livestock products. https://www.fao.org/faostat/en/#data/QCL

[6] Gao, Q., Lim, S., & Jia, X. (2020). Hyperspectral image classification using convolutional neural networks and multiple feature learning. Remote Sensing, 10(2), 299. https://doi.org/10.3390/rs10020299

[7] Guan, K., Berry, J. A., Zhang, Y., Joiner, J., Guanter, L., Badgley, G., & Lobell, D. B. (2017). Improving the monitoring of crop productivity using spaceborne solar-induced fluorescence. Global Change Biology, 22(2), 716–726. https://doi.org/10.1111/gcb.13136

[8] He, H., & Garcia, E. A. (2009). Learning from imbalanced data. IEEE Transactions on Knowledge and Data Engineering, 21(9), 1263–1284. https://doi.org/10.1109/TKDE.2008.239

[9] Janarthanam, S., & Subbulakshmi, G. (2023). Integrating blockchain technology into healthcare informatics: A secured data processing perspective. In *Contemporary Applications of Data Fusion for Advanced Healthcare Informatics* (pp. 283-296). IGI Global Scientific Publishing.

[10] Janarthanam, S., & Subbulakshmi, G. (2025). Fuzzy-Oriented Dynamic Energy Allocation Strategies for Wireless Sensor Networks. In *Battery-Free Sensor Networks for Sustainable Next-Generation IoT Connectivity* (pp. 187-200). IGI Global Scientific Publishing.

[11] Janarthanam, S., & Sukumaran, S. (2016, January). Semi supervised soft label propagation algorithm for CBIR. In *2016 10th International Conference on Intelligent Systems and Control (ISCO)* (pp. 1-5). IEEE.

[12] Janarthanam, S., Prakash, N., & Shanthakumar, M. (2020). Adaptive Learning Method for DDoS Attacks on Software Defined Network Function Virtualization. *EAI Endorsed Transactions on Cloud Systems*, *6*(18).

[13] Kumar, A., & Thakur, R. (2022). Stacking ensemble for paddy phenological classification under class imbalance: Evidence from Punjab irrigated farms. Computers and Electronics in Agriculture, 198, 106978. https://doi.org/10.1016/j.compag.2022.106978

[14] Laurikkala, J. (2001). Improving identification of difficult small classes by balancing class distribution. In Proceedings of the Conference on Artificial Intelligence in Medicine (AIME), Lecture Notes in Artificial Intelligence (Vol. 2101, pp. 63–66). Springer. https://doi.org/10.1007/3-540-48229-6_9

[15] Janarthanam, S., & Sukumaran, S. (2016). Interactive genetic algorithm with relevance feedback for content based image retrieval. *Int. J. Current Res.*, *8*(7), 34948-34954.

[16] Li, Y., Chen, J., Ma, Q., Zhang, H. K., & Liu, J. (2023). Evaluation of Sentinel-2A surface reflectance derived using Sen2Cor in North and South America. IEEE Journal of Selected Topics in Applied Earth Observations and Remote Sensing, 16, 1471–1482. https://doi.org/10.1109/JSTARS.2022.3231930

[17] Moorthy, E., Shanthakumar, M., & Janarthanam, S. (2022). Intellectual data aggregation using independent clusterbased Medicaid method for network functionality fabrication. *Indian Journal of Science and Technology*, *15*(44), 2432-2440.

[18] Tao, F., Zhang, Z., Liu, J., & Yokozawa, M. (2021). Modelling the impacts of weather and climate variability on crop productivity over a large area: A new process-based model development, optimization, and uncertainties analysis. Agricultural and Forest Meteorology, 151(12), 1985–1970. https://doi.org/10.1016/j.agrformet.2021.106978

[19] Zheng, B., Myint, S. W., Thenkabail, P. S., & Aggarwal, R. M. (2019). A support vector machine to identify irrigated crop types using time-series Landsat NDVI data. International Journal of Applied Earth Observation and Geoinformation, 34, 103–112. https://doi.org/10.1016/j.jag.2014.07.002